A Comprehensive Study of Guanosine-5'-triphosphate Hydrolysis by the Bacterial Cell Division Protein FtsZ

by

Andrew Jared Salsburg

Department of Biochemistry
Duke University

Date:_____

Approved:

_____
Harold P. Erickson, Supervisor

_____
Richard Brennan

_____
Margarethe Kuehn

Thesis submitted in partial fulfillment of
the requirements for the degree of
Master of Science in the Department of
Biochemistry in the Graduate School of
Duke University

2018

ABSTRACT

A Comprehensive Study of Guanosine-5'-triphosphate Hydrolysis by the Bacterial Cell Division Protein FtsZ by
Andrew Jared Salsburg

Department of Biochemistry
Duke University

Date:_____

Approved:

_____
Harold P. Erickson, Supervisor

_____
Richard Brennan

_____
Margarethe Kuehn

An abstract of a thesis submitted in partial fulfillment of
the requirements for the degree of
Master of Science in the Department of
Biochemistry in The Graduate School of
Duke University

2018

Abstract

The bacterial protein FtsZ plays a vital role in cytokinesis in prokaryotes as it polymerizes to form an FtsZ ring (Z ring) at the division septum midcell. FtsZ exhibits a GTP hydrolysis activity and attempts have been made to model the kinetics of this process. There is a major discrepancy, however, over the concentration of GTP needed for activity. The dissociation constant (K_D) between wild-type FtsZ protein and GTP was measured to be 30 nM using isothermal titration calorimetry. In contrast, several research groups have reported that GTP hydrolysis required GTP concentrations in the millimolar range. They used Michaelis-Menten kinetics to model the GTP concentration dependence and obtained an apparent binding constant (K_m) in the range of 300-1,000 μM GTP. K_m and K_D are not identical measures of binding given that they differ by the kinetic constant governing catalysis, k_{cat}, but we suggest that a five order of magnitude difference between the values is unprecedented and this was a problem that needed investigating.

My overall goal in this work has been to perform a comprehensive *in vitro* study of the FtsZ GTP hydrolysis activity using an enzyme-coupled regenerating system. With this system rates of GTP hydrolysis by FtsZ are obtained spectrophotometrically. I have confirmed for wild-type FtsZ that GTP hydrolysis rates show little to no dependence on GTP concentrations in the range of 50-3,000 μM, contradicting the high values of K_m reported in some previous studies. Since we have failed to reproduce the high K_m with three different preparations of FtsZ protein, we cannot propose a definitive mechanism for the previous results.

I also measured the GTP hydrolysis of several mutants of FtsZ: E238A, L169R, and FtsZ84 (G105S). I investigated each of these mutants to see if they had a high apparent K_m. FtsZ84 had a low overall hydrolysis rate, but did show a large increase in hydrolysis rates when GTP was increased from 50-3,000 μM. We hypothesize that a lower affinity for GTP is not a Michaelis-Menten K_m, but likely a reflection of a weak binding of GTP by FtsZ84, giving K_D in the millimolar range.

Table of Contents

List of Tables

List of Figures

List of Schemes

List of Abbreviations

Ca *wt* – calcium-assembled wild-type
EDTA – Ethylenediaminetetraacetic acid
EGTA – Ethylene glycol-bis(β-aminoethyl ether)-N,N,N',N'-tetraacetic acid
EM – Electron microscopy
FtsZ – Filamentous temperature sensitive protein Z
GFP – Green fluorescent protein
GDP – Guanosine-5'-diphosphate
GTP – Guanosine-5'-triphosphate
IPTG – Isopropyl β-D-1-thiogalactopyranoside
K_M – Apparent binding constant
K_D – Dissociation constant
LD – Lactate dehydrogenase
NAD^+ – Nicotinamide adenine dinucleotide (oxidized)
NADH – Nicotinamide adenine dinucleotide (reduced)
OD_{600} – Optical density at wavelength of 600 nm
PEP – Phosphoenolpyruvate
PF's – Protofilaments
PIPES – Piperazine-N,N′-bis(2-ethanesulfonic acid)
PK – Pyruvate kinase
PMSF – Phenylmethylsulfonyl fluoride
TEM – Transmission electron microscopy
Tris – Tris(hydroxymethyl)aminomethane
wt – wild-type
Z ring – FtsZ ring

1 Introduction

1.1 Discovery, Homology, and Formation of the Z Ring

The bacterial protein FtsZ plays a vital role in cytokinesis in prokaryotes as it polymerizes to form an FtsZ ring (Z ring) at the division septum midcell.[1] Monomeric FtsZ polymerizes to form protofilaments (PF's), and these PF's then associate with one another making the Z ring. Researchers first visualized FtsZ with immunoelectron microscopy in 1991 showing that it localized to the invaginating septum of dividing *E. coli*.[2] At that time, it was suggested that FtsZ is a cytoskeletal protein in bacteria. Previously, eukaryotic tubulin and actin were thought to have no homologs in bacteria. In 1992 and 1993 three groups independently showed that FtsZ bound and hydrolyzed GTP, and had a 7 amino-acid sequence, GGGTGTG, closely related to the "tubulin signature sequence."[3,4,5] Mukherjee and Lutkenhaus subsequently extended the sequence alignment of FtsZ and tubulins, making a stronger case for homology.[6] In 1998, FtsZ was undeniably identified as a homolog of tubulin when the crystal structures of both proteins showed an identical complex fold.[7,8]

In 1996, the first striking images of the Z ring by fluorescent light microscopy were obtained by immunofluorescence and using FtsZ tagged with GFP.[9,10] Both studies found that the Z rings were present not just at the time of division but through most of the cell cycle. The substructure of the Z ring remained a question, though, since conventional thin-section EM failed to resolve it. In his same year, Erickson *et al*. turned to *in vitro* assembly and found that FtsZ assembled into PF's that average about 125 nm in length with a width of only 5 nm.[11] Figure 1 shows PF's assembled from wild-type (*wt*) *E. coli*

FtsZ, negatively stained with uranyl formate. Later quantitation showed that the Z ring is only three to six PF's wide on average, and these are lost in the granular cytoplasm when using thin-section EM for imaging.[1] This explains why the Z ring could not be resolved by this technique.

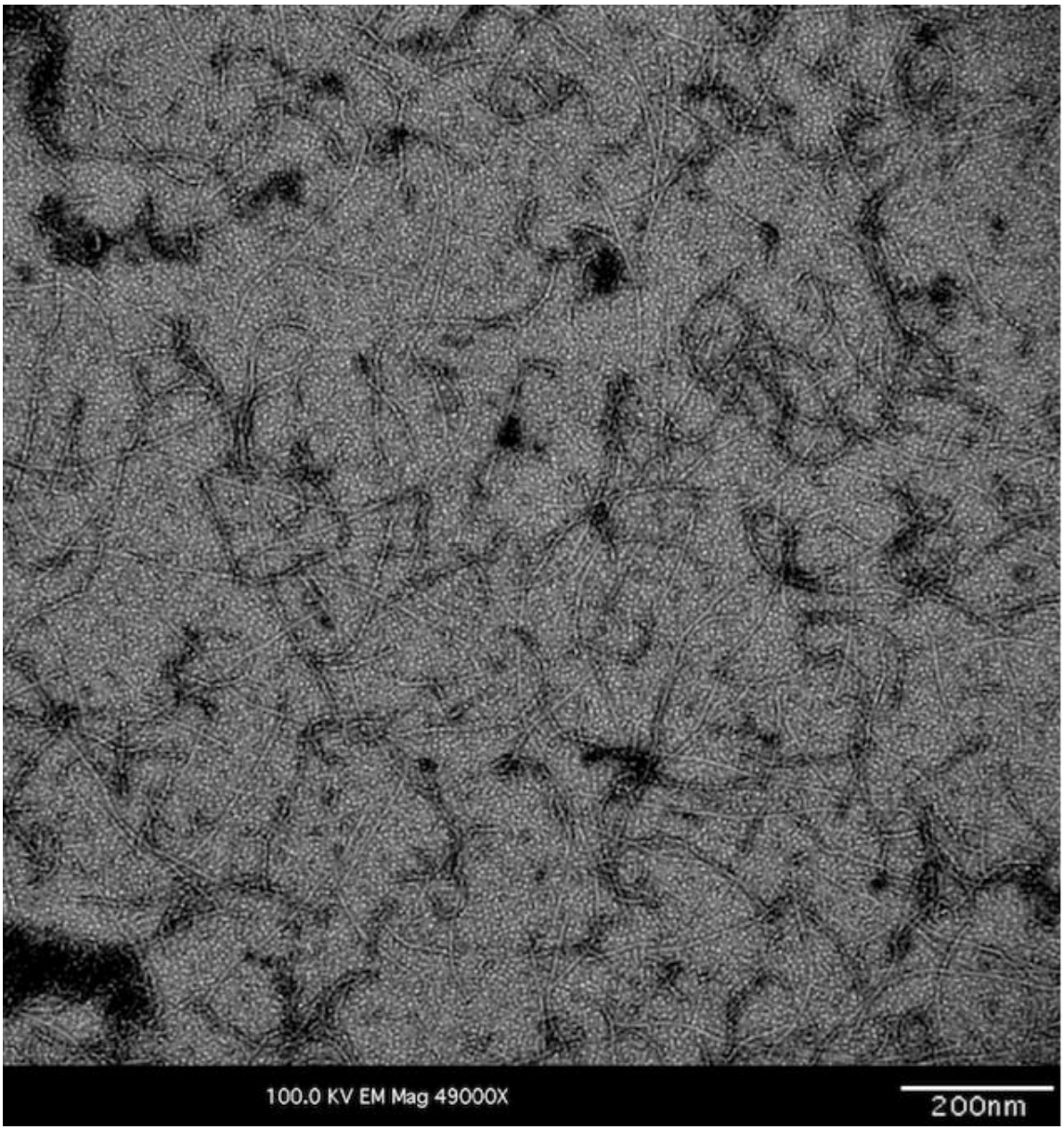

Figure 1 TEM of PF's assembled in 5 µM FtsZ and 1 mM GTP

1.2 GTP binding and Hydrolysis by FtsZ

FtsZ has been shown to possess a GTP binding site with a highly conserved sequence as well as a GTP hydrolysis activity.[3,4,5] The GTP binding site and catalytic residues responsible for hydrolysis are best seen in a study from 2012 in which FtsZ was crystallized in the form of straight, colinear PF's.[12] The nucleotide bound to the top of a subunit of FtsZ, and the T7 loop at the bottom of the subunit above made contact in this structure. This T7 loop is where the catalytic residues responsible for hydrolysis of GTP reside. This study provided a structural mechanism for the fact that GTP hydrolysis only occurs after PF assembly.

Since the hydrolysis activity of FtsZ was first identified, several studies have addressed the question of how GTP concentration affects this activity. The most definitive measure of GTP binding was obtained using isothermal titration calorimetry reporting a K_D of 30 nM and N = 0.81.[13] Additional assays in that study support high affinity binding as well. However, there are several reports in the literature that hydrolysis activity is modulated by GTP concentrations into the micromolar and even millimolar range, suggesting a much lower affinity binding or perhaps a second binding site.

1.2.1 Conflicting Measures of GTP Hydrolysis in FtsZ

The first study to suggest enhanced GTP hydrolysis in high concentrations of GTP reported a linear increase in activity up to 5 mM GTP in pH 7.5 buffer containing 5 mM Mg^{2+} and either 50 or 350 mM K^{+}.[14] This study was conducted in the Erickson lab, but they have been unable to reproduce these results. This study saw a ten-minute lag

before hydrolysis began. That lag was seen in the original discovery papers and was explored in most detail by Mukherjee and Lutkenhaus in 1994 who reported that pretreatment with 1 mM ATP completely eliminated the lag.[6] This will be discussed in greater detail later. Curiously, since 1998, the lag is no longer seen in published papers, although there has been no explanation of what caused it in earlier studies. It may be due to improved purification protocols. Although the lag is no longer seen, a dependence on GTP concentration in the range of 0.1 – 3 mM has been reported by several groups, who have interpreted the concentration for 50% maximum hydrolysis as a Michaelis-Menten K_m.

Table 1 Buffers used in relevant studies for lysis of cells expressing FtsZ, storage of protein, and for assaying GTP hydrolysis rates.

Study	A-Lysis	B-Storage	C-Assay
1-Arjes	pH 8.0 50 mM Tris, 100 mM NaCl, 1 mM EDTA, 1 mM PMSF	-	pH 6.5, 50 mM K^+, 2.5 mM Mg^{++}, 1 mM EGTA
2-Salvarelli	pH 6.5 50 mM PIPES, 5 mM $MgCl_2$, 1 mM EDTA	pH 8.0 50 mM Tris Up to 300 mM KCl 5 mM $MgCl_2$ 1 mM EDTA 10% glycerol	pH 7.5 250 mM K^+, 5 mM Mg^{++}
3-Chen, Erickson	-	pH 7.9 50 mM Tris, KCl 1 mM EDTA 10% glycerol	pH 7.7 100 mM K^+ 5 mM Mg^{++}

As recently as 2015, Arjes *et al*. reported results illustrating an increase in hydrolysis activity over the same range of GTP concentration mentioned above.[15] This group measured hydrolysis activity in buffer C1 from Table 1 above with FtsZ purified

via ammonium sulfate precipitation. Preparation of protein in this experiment called for lysis in buffer A1 from Table 1. This study interprets Micahelis-Menten kinetics for the hydrolysis of GTP by FtsZ and suggests a 1.3 mM K_m for GTP. Back in 1999, Sossong *et al*. reported a much lower K_m of 82 μM.[16] In 2011, Salvarelli *et al*. conducted a careful repeat of the Sossong hydrolysis experiment.[17] The Salvarelli group used buffer C2 from Table 1 with FtsZ purified by cycles of calcium assembly. This purification called for lysis in buffer A2 and subsequent storage in buffer B2 from Table 1. This research group measured a hydrolysis rate between that seen by Sossong and Arjes reporting a K_m of 0.3 mM. A graph of their results is depicted in Figure 2 below. Finally, a recent study by Chen and Erickson showed a moderate increase in the GTP hydrolysis rate over the range of 40-120 μM GTP in buffer C3 from Table 1.[18] This value was not interpreted as a K_m, but may be compared to those values of K_m reported above. In this experiment, protein was stored in buffer B3 from Table 1.

In the present study an attempt was made to reproduce the apparent K_m seen in the studies above, but we failed to find any significant change in GTP hydrolysis rate over the millimolar concentration range. We hypothesize that the discrepancies in K_m reported in previous studies may be due to reversible aggregation of inactivated protein introduced by the different buffers used in storage and handling.

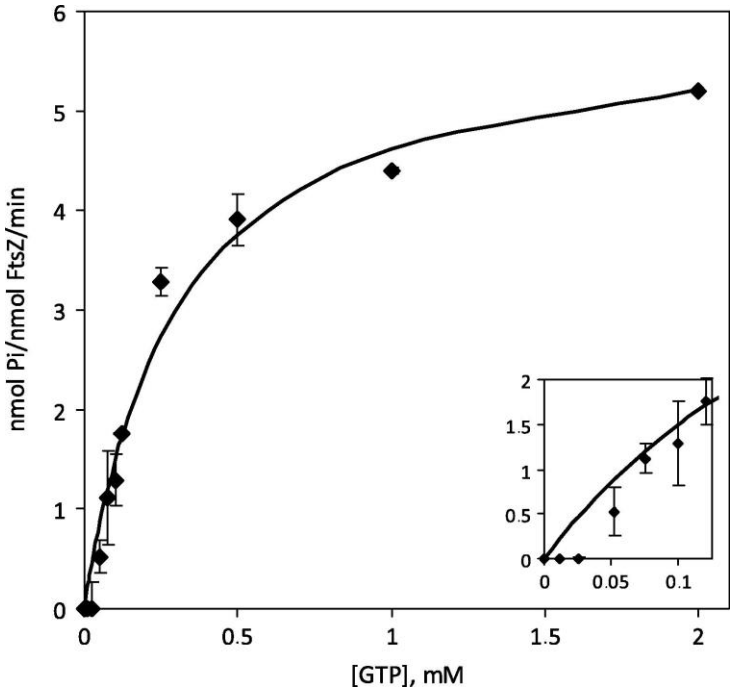

Figure 2 GTPase kinetics of FtsZ. Initial rates were obtained from the slopes of phosphate accumulation curves and fitted to a Michaelis–Menten model with a V_{max} = 6.0 ± 0.4 nmols GTP/nmol FtsZ/min and a K_m = 0.3 ± 0.05 mM (Table 1). Data points are average and standard deviation from three measurements. Inset: expanded view of the plot at low GTP concentrations. Figure and caption from Salvarelli *et al.*[17] Reprinted from Salvarelli *et al*. with permission from John Wiley and Sons.

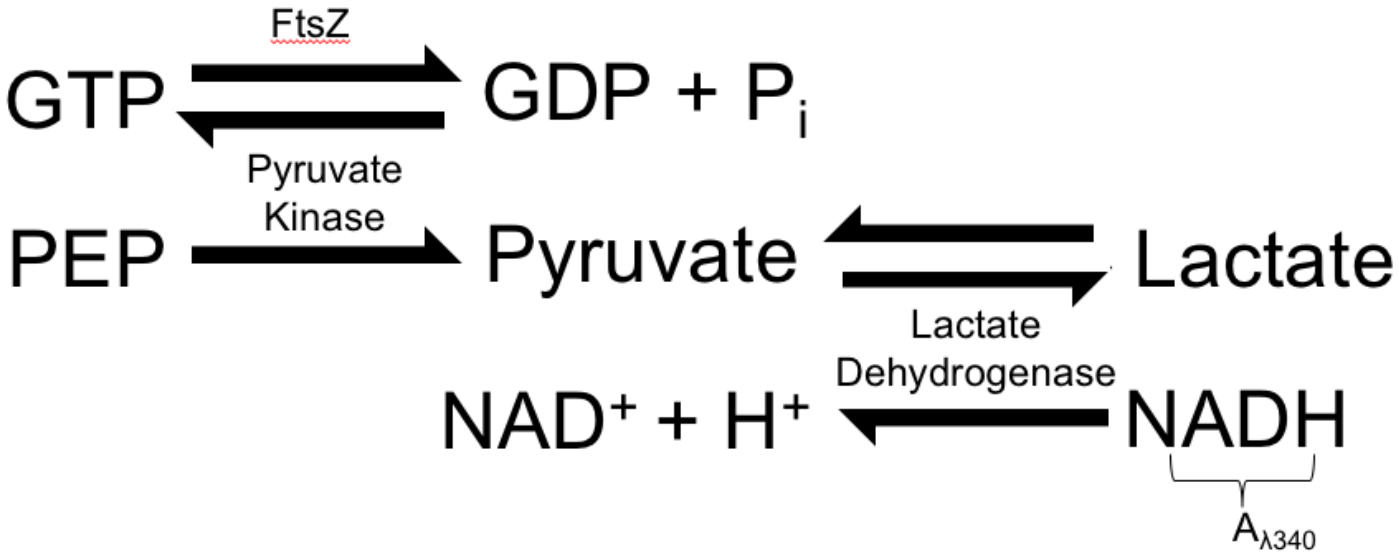

Scheme 1 Visual depiction of the GTP hydrolysis assay using a coupled hydrolysis regenerating system

2 Methods

2.1 The Regenerating System

In work presented here, an enzyme-coupled regenerating assay was used to measure the GTP hydrolysis rates of wild-type FtsZ as well as selected mutants of the protein.[19] In this system, diagrammed in Scheme 1, FtsZ hydrolyzes GTP to GDP. GTP is then regenerated by pyruvate kinase and, in the process, this enzyme converts phosphoenolpyruvate to pyruvate. Lactate dehydrogenase then converts pyruvate to lactate and, in the process, NADH is oxidized to NAD^+. This oxidation is used as a proxy for measuring GTP hydrolysis by FtsZ. Data are obtained spectrophotometrically by monitoring the decrease in absorbance at 340 nm, the wavelength at which NADH absorbs light.

2.1.1 Setting up the Regenerating System

The regenerating system was mixed in a low-volume, quartz cuvette. A solution of 100 µL is all that's needed for accurate measurement of absorbance. 90 µL of this was master mix, 5 µL was FtsZ, and the remaining 5 µL was GTP. The master mix was made such that the final reaction contains 0.6 mM NADH, 1 mM PEP, 23 U/mL PK, and 33 U/mL LD. Stock solutions of PEP and NADH were each made at 100 mM. The concentration of NADH was confirmed spectrophotometrically (ε = 6220 cm^{-1} M^{-1}, path length = 0.3 cm). A mixture of PK/LD was obtained commercially, and the stock concentrations of each enzyme were 800 and 1150 U/mL, respectively. HMK_{100} buffer (pH 7.7, 50 mM Tris, 100 mM KCl, and 5 mM MgAc) was used to achieve the proper final volume of master mix. A 20X stock of protein and GTP were used to initiate the

reaction. The stock concentration of protein was obtained by BCA assay and that of GTP obtained spectrophotometrically ($\varepsilon = 13700\ cm^{-1}\ M^{-1}$). Prior to initiating the experiment, both master mix and GTP were stored in a room temperature water bath. Stocks of protein were stored at 4 °C until just before mixing.

2.1.2 Preparing the Spectrophotometer

The spectrophotometer was turned on and allowed to connect to the computer and warm up. The spectrophotometer was then tuned to 340 nm and placed in kinetics mode which gives an output of absorbance over time. From there, HMK_{100} buffer was used to baseline the instrument. The cuvette was then placed in the instrument and 5 µL of GTP and 5 µL of 20 µM FtsZ added, giving a protein concentration of 1 µM in the starting reaction. GTP concentrations of interest in this experiment were 50, 200, 800, and 3,000 µM.

2.1.3 Initiating Reaction

As quickly as possible, 90 µL of the master mix was added to the cuvette already containing protein and GTP and pipetted up and down, minimizing the introduction of bubbles. The lid was closed, and the start button pressed.

2.1.4 Running the Reaction

This reaction was allowed to proceed for three minutes before more protein was titrated in by adding 5 µL of 20 µM FtsZ and 1 µL of the next highest GTP concentration, and mixing as before. That is, if the initial reaction called for the 60 mM GTP solution, then 1 µL of 16 mM GTP was added here with protein to keep GTP

concentration close to 3 mM upon dilution. Again, this reaction proceeded for three minutes before 5 µL of 20 µM protein and 1 µL of GTP were titrated in as before. This titration was repeated after another three minutes, adding 5 µL of 40 µM protein and 1 µL of GTP, and finally 5 µL of 60 µM protein and 1 µL of GTP after another three minutes. At the end of this procedure, data was obtained for change in absorbance over time at one GTP concentration (50, 200, 800, or 3,000 µM) for five different FtsZ concentrations (1, 1.9, 2.7, 4.3, and 6.45 µM).

2.1.5 Obtaining Hydrolysis Rates

The full time-course was graphed in Microsoft Excel taking the linear portion to be the steady-state hydrolysis rate. The slope of these raw curves is absorbance over time. This was converted into a concentration using Beer's law as follows…

$$X = 1000000\ \mu M * \frac{slope * 60\ min.}{6220 * 0.3} \qquad \text{(Equation 1)}$$

…where X equals a velocity of hydrolysis in µM GTP/min., 6220 is the extinction coefficient of NADH, 0.3 is pathlength of the cuvette in cm, and 1000000 converts units of M to µM, and 60 minutes converts seconds into minutes.

2.2 Protein Purification

2.2.1 Standard Protein Preparation

A 5 mL LB culture of *E. coli* expressing FtsZ in a pET11b vector was grown overnight in LB medium containing 10 g/L NaCl. This was centrifuged the next morning and the pellet resuspended in a baffled flask containing 500 mL of LB. Cells were grown at 37 °C with shaking to an OD_{600} of 0.6-1.0 with 0.8 being ideal before being induced with 2 mM

IPTG. The induced cells were grown at 37 °C with shaking before being centrifuged and resuspended in 10 mL LTK_{50} buffer (pH 7.9, 50 mM Tris, 50 mM KCl, 1 mM EDTA, and 10% glycerol). Cells were lysed using PMSF and powdered lysozyme by adding reagents and placing the solution at -80 °C. Freeze-thaw was carried out three times, and then the sample was sonicated five times for intervals of thirty seconds each. The lysate was centrifuged in a model L8-70 ultracentrifuge in a model 42.1 rotor at 4 °C, 32,000 RPM, for 20 minutes. Ammonium sulfate was added to the supernatant to 30% saturation, and the precipitate was collected by centrifugation at 4 °C, 22,000 RPM, for 20 minutes. Then, the pellet was resuspended in 10 mL of LTK_{50} and allowed to sit at 4 °C overnight. The protein was dialyzed against LTK_{50} and then run on a ResourceQ column. The protein was eluted with a gradient of 0-1 M KCl in LTK_{50}. Fractions taken from the ResourceQ column are combined to give a stock solution of FtsZ.

2.2.2 Crude Protein Preparation

For one experiment, it was necessary to duplicate the protein preparation used in the Lu study mentioned earlier.[14] This followed the same procedure as the standard one up until ammonium sulfate saturation. Where the standard prep calls for saturation of ammonium sulfate of 30%, the crude prep calls for fractionation first with 20% saturated ammonium sulfate. After full dissolution of ammonium sulfate, the solution is spun on the L8-70 ultracentrifuge at 4 °C, 22,000 RPM, for 20 minutes. This pellet was discarded, and the ammonium sulfate was increased to 25% saturation. The same spin was conducted here, and this pellet was resuspended in 10 mL of LTK_{50} buffer.

2.2.3 Calcium Assembly

This assembly procedure, used for select experiments, is a final purification step at the end of the standard preparation. The stock of protein was dialyzed overnight into HMK_{100} buffer that is lacking potassium. In the morning, $CaCl_2$ was added to 10 mM and GTP to 2 mM. This solution was incubated for 5 min at 37 °C forming a white precipitate. The precipitate was centrifuged in the L8-70 ultracentrifuge using rotor 42.1 at 10 °C, 30,000 RPM, for 30 minutes. The supernatant was discarded, and the translucent pellet was resuspended in half the starting volume of HMK_{100}. This solution was stored at 4 °C for 45 minutes. Another spin was conducted using the L8-70 centrifuge at 10 °C, 22,000 RPM, for 20 minutes to remove any insoluble protein. The supernatant was assayed for protein concentration and indicated a recovery of 50-70%.

3 Results

3.1 Obtaining Rates of GTP Hydrolysis in µM GTP/min

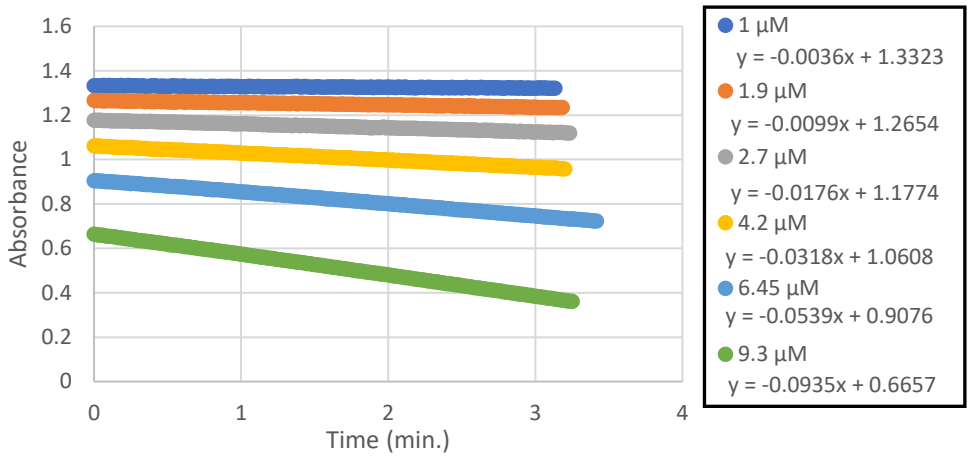

Figure 3 Raw absorbance curves for 1-9.3 µM wild-type FtsZ, 50 µM GTP. The time was reset to zero for each increase in protein concentration. The linear equation fitting each curve is located below its respective legend entry.

There are a number of analytical steps that go into obtaining numerical rates of GTP hydrolysis from the regenerating system. The first step takes place in the experiment where protein is titrated into the reaction while the GTP concentration of that reaction is kept constant. Figure 3 depicts several such curves obtained using this technique at one concentration of GTP. There were a number of protein concentrations ranging from 1 µM to 9.3 µM. A linear decrease in absorbance can be seen for each protein concentration. The slope of the curves in Figure 3 was converted into a concentration using Beer's law. This conversion gives a rate of GTP hydrolysis at one concentration of protein and GTP. For instance, the slope of .0539 seen for 6.45 µM protein at 50 µM GTP in Figure 3 shows a hydrolysis rate of about 28 µM GTP/min using equation 1 above.

3.2 Measures of Turnover at one GTP Concentration

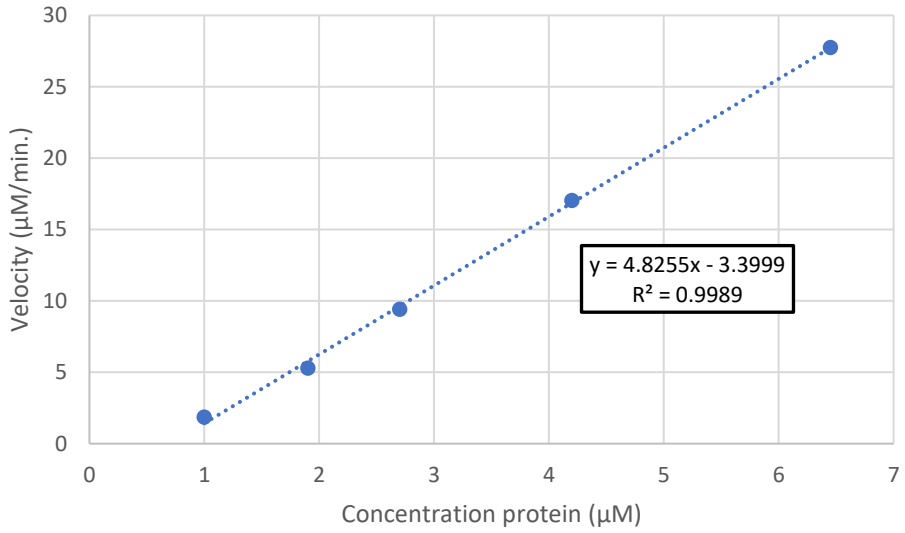

Figure 4 Critical concentration curve for wild-type FtsZ at 50 µM GTP. The velocities were obtained from the slopes of the curves in Figure 3.The slope of the line gives the rate of hydrolysis in GTP per minute per FtsZ.

The next step in the analysis was to plot the hydrolysis velocity versus FtsZ concentration for the full range of concentrations at this particular GTP concentration. Figure 4 shows this plot for the data in Figure 3. This gives a straight line known as a critical concentration curve. The assembly of PF's is known to be cooperative and critical concentration curves in the past have been used to obtain the minimal concentration of FtsZ needed to start PF assembly. Here though, the slope of the critical concentration curve was used to obtain a measure of rate of GTP turnover. Specifically, this slope gives the rate of hydrolysis per FtsZ in polymer. Therefore, Figure 4 shows there are 4.8 molecules of GTP hydrolyzed per FtsZ per minute at a GTP concentration of 50 µM. This experiment and subsequent analysis was completed for four different concentrations of GTP. Those were 50, 200, 800, and 3,000 µM GTP.

3.3 Turnover in Different Preparations of FtsZ

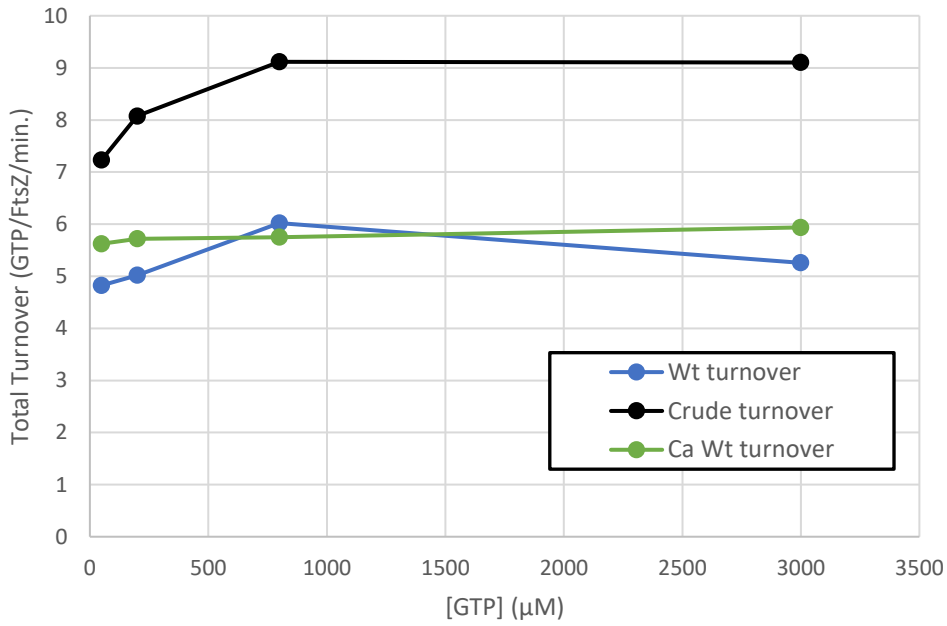

Figure 5 Plot of turnover for the range of GTP concentrations from 50-3,000 μM GTP. Three FtsZ preparations are shown: "normal *wt*," purified by ammonium sulfate and ResourceQ; "crude," purified only by ammonium sulfate; "Ca *wt*," purified using the normal preparation with an additional step of Ca assembly.

Figure 5 depicts the total turnover rates across the range of GTP concentrations for three different protein preparations of *wt* FtsZ. The data points for Figure 5 are given in Tables 2-4. Looking first at the standard preparation of FtsZ, the rate of hydrolysis appears to increase up to 800 μM GTP where it reaches saturation. The crude preparation follows this same trend reaching saturation beyond 800 μM GTP. The calcium-assembled preparation of FtsZ, however, shows little dependence of the rate of hydrolysis on GTP concentration. This indicates saturation across the tested range of GTP. These curves should be compared to that of Salvarelli *et al*. (Figure 2), noting in particular that hydrolysis in that previous study dropped to zero at the lowest GTP concentrations.[17]

Table 2 Turnover rates for standard prep of wild-type FtsZ

[GTP] (μM)	GTP turnover (GTP/FtsZ/min.)
50	4.8
200	5.0
800	6.0
3,000	5.25

Table 3 Turnover rates for crude prep of wild-type FtsZ

[GTP] (μM)	GTP turnover (GTP/FtsZ/min.)
50	7.2
200	8.1
800	9.1
3,000	9.1

Table 4 Turnover rates for calcium-assembled prep of wild-type FtsZ

[GTP] (μM)	GTP turnover (GTP/FtsZ/min.)
50	5.6
200	5.7
800	5.75
3,000	5.9

3.4 Hydrolysis Rates of Selected Mutants

Figure 6 shows the rates of GTP hydrolysis of the standard preparation of wild-type FtsZ and mutants Z84, E238A, and L169R. The goal of Figure 6 is to compare the GTP hydrolysis rates of each mutant back to that of the wild-type protein. E238A hydrolysis rates were seen to be quite similar to that of the wild-type. The L169R mutant showed a large increase in GTP hydrolysis rate from 50-3,000 μM GTP, similar to previous reports of an apparent K_m in the range of 1-2 mM. The Z84 mutant showed two features. First, its overall rate of hydrolysis was quite low over the entire range, consistent with the previous report that its hydrolysis was greatly reduced. Second, the rate increased 5- fold from 50 – 3,000 μM GTP. This is consistent with a K_m of about 1.5

mM, or alternatively a K_D for binding GTP of this magnitude. This will be discussed below.

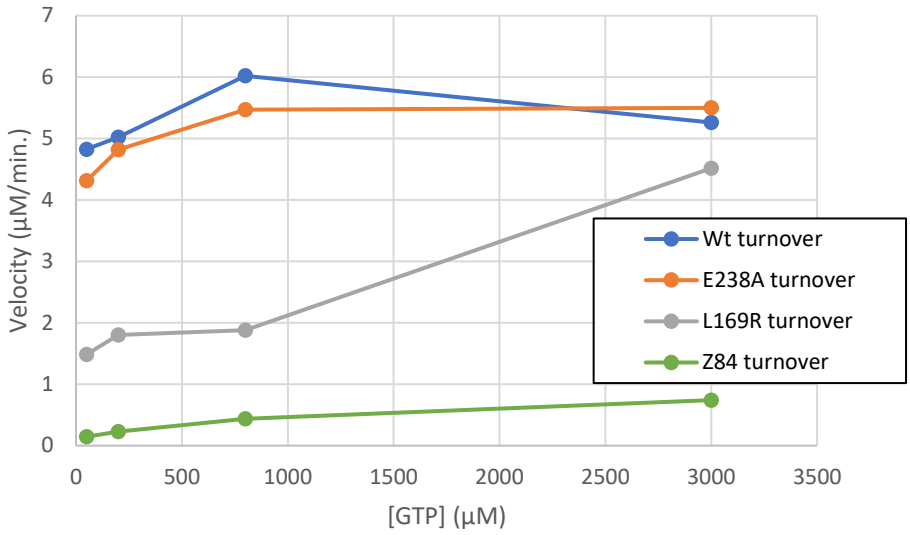

Figure 6 Plot of velocity for selected mutants of FtsZ compared to wild-type protein.

4 Discussion

4.1 Treadmilling and Steady-State Hydrolysis

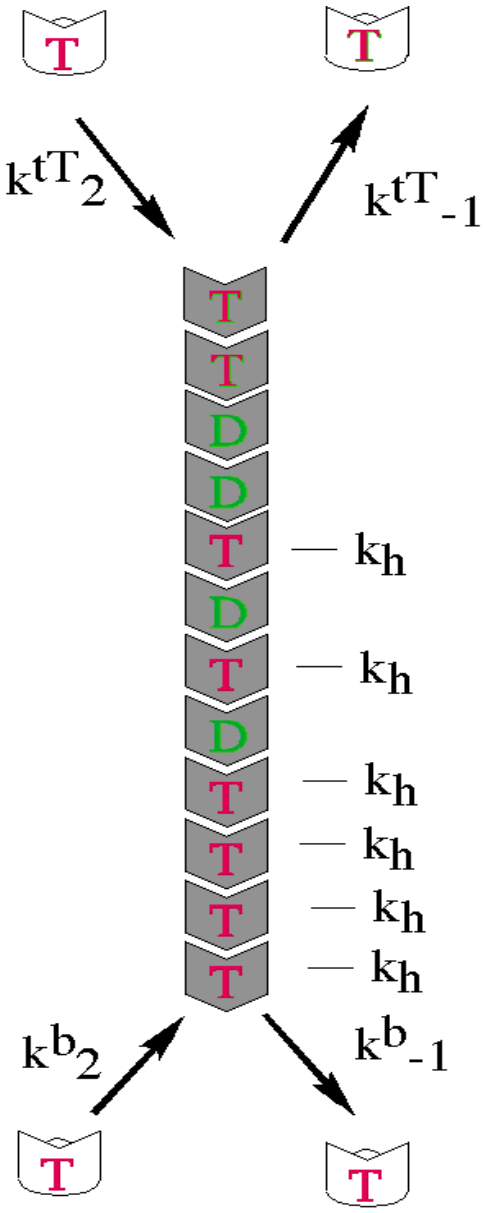

Scheme 2 Model of PF treadmilling

The regenerating assay measures steady-state hydrolysis, a product of PF treadmilling. PF treadmilling is a recently observed phenomenon.[20, 21] Lauren Corbin of

the Erickson lab is trying to model this, and her current picture of how it relates to GTP hydrolysis may be viewed in Scheme 2 above. Subunits of FtsZ containing GTP bind the bottom of a PF and subunits containing GDP are released at the top. Hydrolysis happens stochastically for subunits anywhere in the PF. Importantly PF's do not fragment at the internal GDP sites, and nucleotide does not exchange into the PF. Subunits can exchange nucleotide only when released at the top. Once a subunit has exchanged its GDP for GTP it can add on to the bottom. Thus, steady-state GTP hydrolysis is measuring the rate at which GDP bound subunits are dissociating at the top, exchanging nucleotide in solution and re-associating at the bottom. Therefore, GTP hydrolysis rates are measures of steady-state subunit exchange.

4.2 Effects of Purification on GTP Hydrolysis Rates

The crude preparation referenced in Figure 5 is one that has been used historically to purify FtsZ protein and is still used today by some labs. The standard preparation is one that is most commonly used to purify FtsZ protein in the Erickson lab and was indeed the method used to purify not only wild-type protein, but each of the mutants in Figure 6. The calcium-assembly in Figure 5 is an FtsZ-specific protein purification procedure. In calcium assembly, the sample of FtsZ is made to assemble into PF's in the presence of both calcium and GTP. Those protofilaments are spun out of solution via ultracentrifuge and allowed to disassemble before one last spin to remove still-assembled PF's from stock solution. This procedure removes any inactive protein along with contaminating impurities.

In analyzing the data in Figure 5, the main concern was comparing the results obtained here to those obtained by Salvarelli *et al*. and Arjes *et al*. in which those groups reported values of K_m of 0.3 and 1.3 mM, respectively.[15,17] These were the two studies that motivated the present study because the K_m they deduced was five orders of magnitude higher than the K_D for GTP binding determined by Huecas *et al*.[13]

Figure 5 illustrates that, following the final step of calcium assembly, *wt* FtsZ showed no variation in the rate of hydrolysis over the range from 50-3,000 μM GTP. Thus, there is no indication of a K_m in this range. There was, however, an increase in hydrolysis from 50-800 μM GTP for both the standard and crude preparations. We suggest that this dependence may be due to contaminating GTPase proteins that were removed by the final calcium assembly step. Thus, from our work we see no indication of a millimolar K_m for wild-type FtsZ. An important difference in Figure 5 and the curves of Salvarelli *et al*. and Arjes *et al*, is that their curves approached zero at 50 μM GTP (See Figure 2), whereas Figure 5 showed rates of hydrolysis only slightly below saturation.[15,17] We sought to explain their apparent high K_m suggesting that it may be due to reversibly aggregated FtsZ protein revived by a hydrotrope effect at millimolar GTP concentrations.[22]

4.3 The Hydrotrope Effect

A hydrotrope is typically used in industrial contexts as a bridge between aqueous and organic phases because it possesses features that allow the two otherwise immiscible layers to mix. However, this past year, Patel *et al*. presented a careful study in which they showed ATP may behave as a biological hydrotrope.[22] In one experiment, they observed

the aggregation of chicken egg white at 60 °C under a number of different conditions. At this temperature, chicken egg white aggregates and turns the previously clear solution turbid. They showed that ATP chelated with magnesium could block the egg white aggregation – 3 mM ATP-Mg blocked 50%, and 10 mM was sufficient to block aggregation completely. Controls of sodium chloride at the same ionic strength of ATP showed that the ionic character of ATP did not cause aggregation, nor could the prevention of aggregation be attributed to any sort of hydrolysis because a non-hydrolysable analog had comparable hydrotropic effect to ATP. Most importantly for our study is the fact that Patel *et al*. found that GTP is just as active a hydrotrope as ATP.[22]

4.3.1 The Hydrotrope Effect in FtsZ

The hydrotrope effect may actually be used to explain a previously ambiguous result obtained in measuring the GTP hydrolysis rates of FtsZ.[5,6] In 1993, Mukherjee *et al*. reported rates of hydrolysis in picomoles of phosphate released.[5] Strangely, the hydrolysis activity was reported to be enhanced about four-fold when the FtsZ was preincubated for 90 minutes in 5 mM ATP. Preincubation with ATP also eliminated a mysterious lag in the onset of hydrolysis. Mukherjee *et al*. reported their finding but did not suggest a mechanism for it.[5] We believe they had evidence of the hydrotrope effect, but this was not understood in a biological context until very recently.[22] Importantly, FtsZ is known to form aggregates. We suggest that the FtsZ in the preparation of Mukherjee *et al*. was largely aggregated and inactive, and ATP activated GTP hydrolysis serving as a hydrotrope by solubilizing those aggregates allowing for greater bulk activity.

We initially thought that a hydrotrope effect may be occurring in the experiments of Salvarelli *et al*. and Arjes *et al*. However, a problem with this suggestion is that these groups did not report a lag before hydrolysis began. If GTP is acting as a hydrotrope, solubilizing the aggregated FtsZ should require time after addition of GTP. A lag was seen the earlier work of Mukherjee *et al*. and was eliminated by preincubation with ATP.[5,6] Salvarelli *et al*. and Arjes *et al*. did not report detailed kinetics of hydrolysis, but it seems unlikely that they observed a significant lag before hydrolysis began.[15,17] Overall, we cannot explain the apparent K_m of Salvarelli *et al*. and Arjes *et al*, because we have failed to duplicate their experimental data. None of our preparations of wild-type FtsZ showed a K_m in the millimolar range.

4.4 Kinetics of Hydrolysis in FtsZ Mutants

Three mutants were selected for characterization of GTPase. FtsZ84 (G105S) is one of the first temperature sensitive mutants of FtsZ to be discovered. The three studies discovering FtsZ as a GTPase related to tubulin all reported that Z84 protein bound GTP much more weakly than wild-type.[3,4,5] Our measure of GTPase showed a significant rise from 50-3,000 µM GTP. This might be interpreted as a K_m, but we suggest that it is probably a measure of a reduced binding affinity of Z84 for GTP, giving a K_D in the millimolar range. This would explain why FtsZ84 shows compromised assembly and activity *in vitro*,[15] but fully functions for FtsZ *in vivo* at the permissive 30 °C. Most *in vitro* experiments have been done at 1 mM GTP or less, while the *in vivo* concentration of GTP is known to be 3 mM or greater. Future experiments by isothermal titration calorimetry are needed to confirm the K_D.

E238A was selected because Yang *et al*. reported it to have a K_m 20 times higher than *wt* FtsZ.[21] However, our measurements showed that its hydrolysis rate was identical to that of *wt* FtsZ, with no indication of a millimolar K_m. L169R was discovered as a gain of function mutation of FtsZ that was able to bypass the need for ZipA and was immune to the phage toxin Kil.[23,24] It was reported to have a reduced GTP hydrolysis activity *in vitro* that was attributed to possible bundling. Our data showed a strong increase in hydrolysis rate with increasing GTP concentration, which might be related to the elusive K_m. L169R is not in contact with the GTP, but it is on a nearby loop. It needs to be determined if the mutation weakens the binding of GTP.

5 Conclusion

The aim of this study was to provide some clarity in the apparent K_m of FtsZ for GTP in hydrolysis given the immense discrepancies that exist in the literature using a regenerating assay to measure hydrolysis rates of wild-type FtsZ protein. I also aimed to measure the GTP hydrolysis rates of mutants E238A, L169R, and Z84 (G105S) with special focus on Z84.

We completely failed to reproduce the strong dependence on GTP concentration, in spite of using protein purification and assay conditions close to those reported. It remains a mystery why some labs have seen this concentration dependence.

With regards to the mutants tested, E238A appears to be too similar to the wild-type to warrant further characterization. L169R yielded interesting results that need to be characterized further. Preliminary data with Z84, however, allowed us to hypothesize that this mutant has a true weak binding to GTP, consistent with measures of binding in previous studies. Future studies using isothermal titration calorimetry as well as EM will be needed to confirm this.

6 Supplement

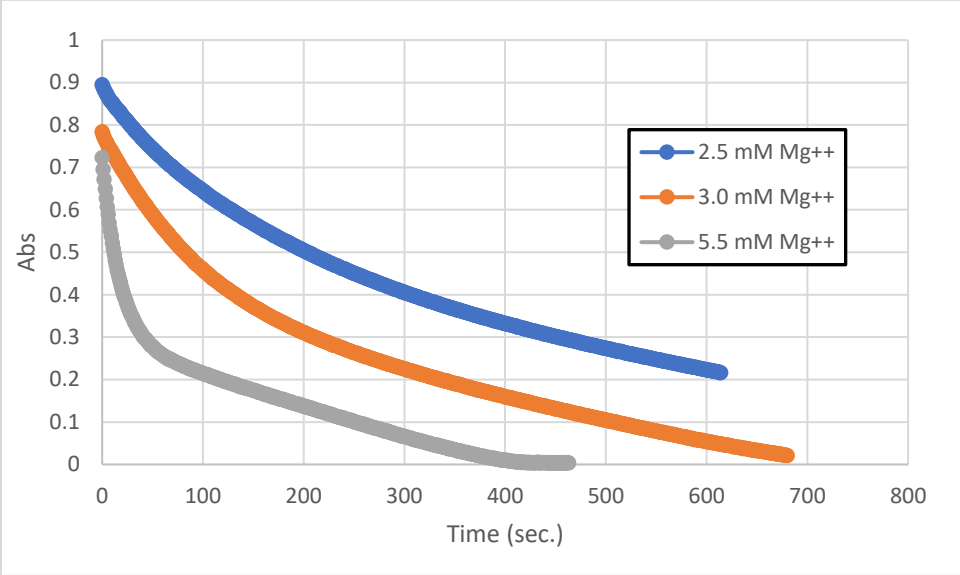

Supplemental Figure 1 5 µM FtsZ, 3 mM GTP, and different concentrations of magnesium ion present in buffer as indicated by the legend.

Supplemental Figure 1 above represents an interesting discovery on the regenerating system itself that didn't quite fit into the story told by the other data obtained in this study. In performing many assays using the regenerating system, I noticed that there is a level of GDP initially present in GTP solutions that shows itself at high concentrations of GTP. When GDP is present at start, it is rapidly converted back to GTP. This can be seen in the gray curve present in Supplementary Figure 1. The initial burst upon initiation of measurement represents the conversion of GDP to GTP. Upon conversion of all the GDP, the curve quickly established linearity (steady-state hydrolysis) before running out of NADH and flatlining. With the same amount of GDP present the blue and orange curves did not show this pattern. There wasn't a sequential conversion of GDP and establishment of steady-state hydrolysis. Instead, there was one

smooth curve that never plainly showed the features of either kinetic regime. As is indicated by the legend, the concentration of magnesium ion was seen to be the cause of the differences between each of these curves. When magnesium was equal to or lower in concentration than GTP, the regenerating system did not behave well, never establishing steady-state hydrolysis. When magnesium was in excess of GTP, however, the regenerating system had no problem converting all GDP back to GTP before establishing steady-state hydrolysis afterward. It is well known that nucleotide triphosphates chelate magnesium.[25] Therefore, it was concluded that for the regenerating system to work properly, an excess of magnesium had to be present over GTP.

References

[1] Erickson, H. P., Anderson, D.E., Osawa, M. (2010). "FtsZ in Bacterial Cytokinesis: Cytoskeleton and Force Generator All in One." Microbiol Mol Biol Rev 74(4): 504-528.

[2] Bi, E. F. and J. Lutkenhaus (1991). "FtsZ ring structure associated with division in Escherichia coli." Nature 354(6349): 161-164.

[3] Boer, P., Crossley, R., Rothfield, L. (1992). "The essential bacterial cell-division protein FtsZ is a GTPase." Lett. Nature 359: 254-256.

[4] RayChaudhuri, D. and J. T. Park (1992). "Eschericia coli Cell-Division Gene FtsZ Encodes a Novel GTP-Binding Protein" Lett. Nature 359: 251-254.

[5] Mukherjee, A., Dai, K., Lutkenhaus, J. (1993). "Escherichia coli cell division protein FtsZ is a guanine nucleotide binding protein." Biochemistry 90: 1053-1057.

[6] Mukherjee, A. and J. Lutkenhaus (1994). "Guanine Nucleotide-Dependent Assembly of Ftsz into Filaments." Journal of Bacteriol. 176(9): 2754-2758.

[7] Lowe, J. and L. A. Amos (1998). "Crystal structure of the bacterial cell-division protein FtsZ." Nature 391(6663): 203-206.

[8] Nogales, E., Wolf, S. G., Downing, K. H. (1998). "Structure of the alpha beta tubulin dimer by electron crystallography." Nature 391(6663): 199-203.

[9] Levin, P. A. and R. Losick (1996). "Transcription factor Spo0A switches the localization of the cell division protein FtsZ from a medial to a bipolar pattern in Bacillus subtilis." Genes & Development **10**(4): 478-488.

[10] Ma, X., Ehrhardt, D. W., Margolin, W. (1996). "Colocalization of cell division proteins FtsZ and FtsA to cytoskeletal structures in living Escherichia coli cells by using green fluorescent protein." Proc. of the Natl Acad of Sci 93(23): 12998-13003.

[11] Erickson, H. P., Taylor, D. W., Taylor, K. A., Bramhill, D. (1996). "Bacterial cell division protein FtsZ assembles into protofilament sheets and minirings, structural homologs of tubulin polymers." Proc. of the Natl Acad of Sci 93(1): 519-523.

[12] Matsui, T., Yamane, J., Mogi, N., Yamaguchi, H., Takemoto, H., Yao, M., Tanaka, I. (2012). "Structural reorganization of the bacterial cell-division protein FtsZ from Staphylococcus aureus." Acta Crystallogr D Biol Crystallogr 68(Pt 9): 1175-1188.

[13] Huecas, S., Schaffner-Barbero, C., Garcia, W., Yebenes, H., Palacios, J. M., Diaz, J.F., Menendez, M., Andreu J.M. (2007). “The Interactions of Cell Division Protein FtsZ with Guanine Nucleotides.” J. Biol. Chem. 282(52): 37515-37528.

[14] Lu, C. L., Stricker, J., Erickson, H. P. (1998). "FtsZ from Escherichia coli, Azotobacter vinelandii, and Thermotoga maritima - Quantitation, GTP hydrolysis, and assembly." Cell Motility and the Cytoskeleton 40(1): 71-86.

[15] Arjes, H. A., Lai, B., Emelue, E., Steinbach, A. , Levin, P. A. (2015). "Mutations in the bacterial cell division protein FtsZ highlight the role of GTP binding and longitudinal subunit interactions in assembly and function." BMC Microbiol 15(209): 209.

[16] Sossong, T. M., Brigham-Burke, M. R., Hensley, P., Pearce, K. H. (1999). "Self-Activation of Guanosine Triphosphatase Activity by Oligomerization of the Bacterial Cell Division Protein FtsZ." Biochemistry 38(45): 14843-14850.

[17] Salvarelli, E., Krupka, M. , Rivas, G. , Vicente, M. , Mingorance, J. (2011) "The Cell Division Protein FtsZ from Streptococcus pneumoniae Exhibits a GTPase Activity Delay." FEBS Lett 585: 3880-3883.

[18] Chen, Y. and H. P. Erickson (2009). "FtsZ filament dynamics at steady state: subunit exchange with and without nucleotide hydrolysis." Biochemistry 48(28): 6664-6673.

[19] Ingerman, E. and J. Nunnari (2005). "A continuous, regenerative Coupled GTPase Assay for Dynamin-related proteins." Methods Enzymol 404: 611-619.

[20] Bisson-Filho, A. W., Hsu, Y., Squyres, G., Kuru, E., Wu, F., Jukes, C., Sun, Y., Dekker, C., Holden, S., VanNieuwenhze, M. S., Brun, Y. V., Garner, E. C. (2017). "Treadmilling by FtsZ filaments drives peptidoglycan synthesis and bacterial cell division." Science 355(6326): 739-743.

[21] Yang, X., Lyu, Z., Miguel, A., McQuillen, R., Huang, K. C., Xiao, J. (2017). "GTPase activity-coupled treadmilling of the bacterial tubulin FtsZ organizes septal cell wall synthesis." Science 355(6326): 744-747.

[22] Patel, A., Malinovska, L., Saha, S., Wang, J., Alberti, S., Krishnan, Y., Hyman, A. A. (2017). "ATP as a biological hydrotrope." Science 356: 753-756.

[23] Haeusser, D. P., Hoashi, M., Weaver, A., Brown, N., Pan, J., Sawitzke, J. A., Thomason, L. C., Court, D. L., Margolin, W. (2014). "The Kil peptide of bacteriophage lambda blocks Escherichia coli cytokinesis via ZipA-dependent inhibition of FtsZ assembly." PLoS Genet **10**(3): e1004217.

[24] Haeusser, D. P., V. W. Rowlett, W. Margolin. (2015). “A mutation in Escherichia coli ftsZ bypasses the requirement for the essential division gene zipA and confers resistance to FtsZ assembly inhibitors by stabilizing protofilament bundling.” Mol Microbiol 97:988-1005.

[25] Wilson, J. E. and A. Chin (1991). "Chelation of divalent cations by ATP, studied by titration calorimetry." Analytical Biochemistry 193(1): 16-19.